

# Improvement of the electrochemical properties of “as-grown” boron-doped polycrystalline diamond electrodes deposited on tungsten wires using ethanol

Reinaldo F. Teófilo · Helder J. Ceragioli ·  
Alfredo C. Peterlevitz · Leonardo M. Da Silva ·  
Flavio S. Damos · Márcia M. C. Ferreira ·  
Vitor Baranauskas · Lauro T. Kubota

Received: 5 March 2007 / Accepted: 26 March 2007 / Published online: 15 May 2007  
© Springer-Verlag 2007

**Abstract** The electrochemical properties of boron-doped diamond (BDD) polycrystalline films grown on tungsten wire substrates using ethanol as a precursor are described. The results obtained show that the use of ethanol improves the electrochemistry properties of “as-grown” BDD, as it minimizes the graphitic phase upon the surface of BDD, during the growth process. The BDD electrodes were characterized by Raman spectroscopy, scanning electronic microscopy, cyclic voltammetry (CV), and electrochemical impedance spectroscopy (EIS). The boron-doping levels of the films were estimated to be  $\sim 10^{20}$  B/cm<sup>3</sup>. The electrochemical behavior was evaluated using the Fe(CN)<sub>6</sub><sup>3-/4-</sup> and Ru(NH<sub>3</sub>)<sub>6</sub><sup>3+/2+</sup> redox couples and dopamine. Apparent heterogeneous electro-transfer rate constants  $k_{app}^0$  were determined for these redox systems using the CV and EIS techniques.  $k_{app}^0$  values in the range of 0.01–0.1 cm s<sup>-1</sup> were observed for the Fe(CN)<sub>6</sub><sup>3-/4-</sup> and Ru(NH<sub>3</sub>)<sub>6</sub><sup>3+/2+</sup> redox couples, while in the special case of dopamine, a lower  $k_{app}^0$  value of 10<sup>-5</sup> cm s<sup>-1</sup> was found. The obtained results showed that the use of CH<sub>3</sub>CH<sub>2</sub>OH (ethanol) as a carbon source constitutes a promising alternative for manufacturing BDD electrodes for electroanalytical applications.

**Keywords** Boron-doped diamond electrodes · Ethanol · Cathodic pretreatment · EIS

## Introduction

The development of chemical and biological sensors of high sensitivity and stability has attracted great attention to electroanalytical applications of boron-doped polycrystalline diamond electrodes. Boron-doped diamond (BDD) has demonstrated to be an attractive material for electroanalytical applications, in view of its unique properties such as robustness, chemical inertness, resistance to electrode fouling, wide potential window, and low background currents [1–3].

However, several factors influence the electrical conductivity within BDD films and the charge transfer rates across the BDD/solution interface [4]. As a result, the electrochemical properties are influenced mainly by: (1) doping type and level, (2) morphology features (e.g., grain boundaries and point defects), (3) nondiamond impurity content, (4) crystallographic orientation, and surface group functionalities (H vs O). The extent of each one of these factors affecting the electrochemical response depends significantly on the reaction mechanism for the particular redox system [4–7].

The carbon source can be an important variable in the characteristics of BDD of electroanalytical interest, although methane is the most often employed carbon source [1, 2, 4, 7, 8].

Stoneham et al. [9] showed, using a phenomenological model, how the growth of BDD films from a C–H–O mixture can lead to the formation of high-quality materials if the reagent concentration was optimized. According to this author [9], the presence of oxygen in the gas phase ties up

R. F. Teófilo · F. S. Damos · M. M. C. Ferreira · L. T. Kubota  
Instituto de Química, Universidade Estadual de Campinas,  
P.O. Box 6154, 13084-971 Campinas, SP, Brazil

H. J. Ceragioli · A. C. Peterlevitz · V. Baranauskas (✉)  
Faculdade de Engenharia Elétrica e Computação,  
Universidade Estadual de Campinas,  
Av. Albert Einstein 400,  
13083-852 Campinas, SP, Brazil  
e-mail: vitor.baranauskas@gmail.com

L. M. Da Silva  
Departamento de Química-FACESA,  
Universidade Federal dos Vales do Jequitinhonha e Mucuri,  
39100-000 Diamantina, MG, Brazil

a proportion of the available carbon in the form of CO, which reduces the flux of reactive carbonaceous groups to the surface. Experiments showed that using a microwave-plasma-enhanced chemical vapor deposition (CVD) reactor and small amounts of oxygen in the methane and hydrogen mixture may increase the rate of the film growth but also the impurity content [10, 11]. On the other hand, Baranauskas et al. [12, 13] have obtained a high-quality diamond deposited on silicon or tungsten with ethanol and hydrogen using hot-filament-assisted CVD (HFCVD), with a low quantity of reactive carbonaceous groups. Indeed, several different reports [14, 15] have pointed out that ethanol as a carbon source to grow diamonds comprises a good alternative in obtaining high-quality diamond films. However, only a few papers have been devoted to obtain BDD films from alcohol (ethanol or methanol) [16–18].

The diamond growth using different carbon sources apart from methane is seldom exploited in electrochemical researches, probably because of the difficulty in obtaining a material that presents the required qualities, because not always a conducting diamond originated from the C–H–O mixture supplies all the characteristics required for the electrochemical applications. The ethanol was chosen because of its characteristic in decreasing the graphitic phase during growing. This characteristic is extremely important in electrochemistry because film growth from other sources require graphite removing by different drastic methods, chemical [4, 8] or electrochemical [8], after growing.

The presence of nondiamond carbon, mostly constituted by graphitic domains, could play the role of electrocatalytic centers and bring functional groups on the electrode surface [8]. However, those Csp<sup>2</sup> impurities tend to be formed in the grain boundaries and defects during the CVD process [7]. The magnitude of the background current, working potential window, and the voltammetric features are all sensitive to the presence of nondiamond (amorphous or graphitic) carbon impurities [2, 4]. In a very general way, adsorbed contaminants can either block specific surface sites or increase the electron-tunneling distance for redox analytes [8].

The objective of this study is the investigation of the electrochemical properties of “as-grown” BDD films prepared using ethanol, applying different in situ (cyclic voltammetry [CV] and electrochemical impedance spectroscopy [EIS]) and ex situ (scanning electronic microscopy [SEM] and Raman) techniques, showing that the graphite should be responsible for the decrease in the electroactivity of the BDD electrode.

## Experimental

### Diamond deposition

Polycrystalline BDD films were produced in a previously described all-quartz cylindrical HFCVD reactor [19]. A

boron-doping source was performed dissolving solid B<sub>2</sub>O<sub>3</sub> in ethanol in the liquid reservoir before starting up the reactor. Tungsten wires with a diameter of 238 μm and length of 30 mm were used as substrates. The wires were mounted onto a polished silicon wafer placed below the hot filament and parallel to the central axis of the filament coil. Deposition temperatures were measured by a thermocouple underside of the silicon wafer. Before deposition, the tungsten wires were dipped in a colloidal mixture of diamond dust (0.25 μm in diameter) dispersed by ultrasonic vibration in *n*-hexane. This ‘seeding’ is a used procedure to increase the nucleation density of diamond films. The diamond films were deposited employing a mixture of ethanol (CH<sub>3</sub>CH<sub>2</sub>OH) vapor diluted in hydrogen gas (99.5% vol) at a volumetric flow rate of 100 standard cm<sup>3</sup> per min, regulated by precision mass flow meters, and a total pressure kept at 20 Torr. We classified our samples in two typical types, A and B, according to their respective deposition temperatures: Type A were grown at deposition temperatures set at 1,050 K for 30 h, and type B were grown at 910 K for 35 h. The boron doping concentrations, estimated using Mott–Schottky plots, were  $\sim 2.9 \times 10^{20}$  and  $\sim 4.0 \times 10^{18}$  B cm<sup>-3</sup> (5,000 ppm or 0.5% B/C) for type A and B, respectively. Electric connections were placed on both types by wire wrapping a nickel–chromium wire and sealing with silver paint. The electrodes were insulated by a Teflon band and epoxy resin and then inserted into polypropylene tubes, exposing only the diamond area on the top of the electrodes for the electrochemical studies.

### BDD electrode pretreatments

BDD films “as grown” received a mild cathodic treatment in 1.0 mol L<sup>-1</sup> HNO<sub>3</sub>. The cathodic treatment, a modified treatment presented by Marken et al. [20], was carried out by cycling the potential in the range from 0 to -4 V (vs a saturated calomel electrode [SCE]) for at least three times. We have observed that this pretreatment is also effective for recovery of diamond electrodes after extensive times of analysis.

### BDD film characterizations

The BDD films were characterized using different in situ and ex situ techniques. For the ex situ characterization, the scanning electron microscopy (SEM) was used to examine the film morphology using a JEOL 6360–LV instrument. The Raman spectroscopy technique was employed to investigate the structural properties of the BDD films at ambient temperature ( $\sim 25$  °C) using an Jobin Yvon T64000 Raman spectrometer, employing an Argon laser for excitation (514.5 nm wavelength) at a laser power of about 6 mW.

**Electrochemical studies** The samples were characterized using the CV and the EIS techniques.

**CV study** Voltammograms were obtained using 5 ml of the supporting electrolyte containing different electroactive compounds ( $\text{Fe}(\text{CN})_6^{3-/4-}$ ,  $\text{Ru}(\text{NH}_3)_6^{3+/2+}$  and dopamine) with a concentration of  $1.0 \times 10^{-3} \text{ mol L}^{-1}$ . CV was performed at different scan rates, between 0.02 and  $0.1 \text{ V s}^{-1}$ . In all cases, the potential range was cycled for three times, and the last cycle was recorded. Pure  $\text{N}_2$  was bubbled through the sample solutions for 5 min before each measurement.

**Quasi-steady polarization curves** In the special case of dopamine, the Quasi-steady polarisation curves (QSPC) were carried out in a range of 200 mV in relation to the open circuit potential (equilibrium potential). The experimental data were corrected for ohmic drop. The supporting electrolyte was  $1 \text{ mol L}^{-1}$  KCl solution, and the dopamine concentration was  $1 \times 10^{-3} \text{ mol L}^{-1}$ .

**EIS study** In all cases, the electrochemical investigation in the frequency domain was carried out by applying a d.c. potential at the open circuit potential. Impedance spectra were recorded covering the 10-mHz to 100-kHz frequency interval. To ensure the linearity of the electrode response, a small amplitude sine wave (5 mV [p/p]) was used throughout. As required by the linear system theory, validation of the EIS data was performed applying the Kramers–Kronig test using a software acquired from the AUTOLAB electrochemical system. The equivalent circuit, EC, proposed in the literature [3, 7] for the BDD electrode in the presence of diffusion control, was applied to fit the impedance data using the EQUIVCRT program elaborated by Boukamp [21]. Pure  $\text{N}_2$  was bubbled through the sample solutions for 5 min before each measurement.

The electrochemical studies were carried out using an all-glass electrochemical cell ( $10 \text{ cm}^3$ ). A platinum wire was used as a counter electrode, and all potentials were recorded against a SCE. All measurements were carried out at  $25 \text{ }^\circ\text{C}$ . An AUTOLAB (Eco Chemie, The Netherlands) electrochemical system (GPES), PGSTAT-30 model, was used throughout.

## Solutions

In both cases, the electrochemical behavior associated with the electron-transfer reaction at the BDD/solution interface was investigated using aqueous solutions containing one of the  $\text{Fe}(\text{CN})_6^{3-/4-}$  (Aldrich) or  $\text{Ru}(\text{NH}_3)_6^{3+/2+}$  (Aldrich) redox couples or dopamine (Acros). The supporting electrolytes in each case were composed of  $1 \text{ mol L}^{-1}$  KCl (Synth),  $1 \text{ mol L}^{-1}$   $\text{HNO}_3$  (Merck), or  $0.1 \text{ mol L}^{-1}$   $\text{H}_2\text{SO}_4$  (Merck) solutions.

All reagents were analytical grade without additional purification. All solutions were prepared with ultra pure water from a Milli-Q® purification system ( $>18 \text{ M}\Omega \text{ cm}$ ).

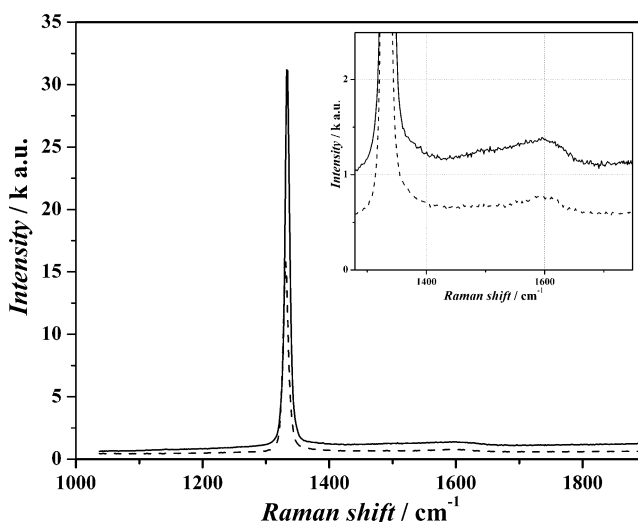
## Results and discussion

### Raman spectroscopy

Diamond films synthesized by CVD with methane and other carbon sources, in many times, contain graphitic carbon [4, 7]. Raman spectroscopy is one of the best tools to assess the qualities of BDD films because graphitic carbon has a distinctly different Raman peak that is more intense than the diamond peak, thus allowing a small amount of graphitic carbon to be recognized in BDD films. Figure 1 shows the typical Raman spectra of the “as-grown” samples. There is a single sharp peak at  $1,330 \text{ cm}^{-1}$  that corresponds to the C–C  $\text{sp}^3$  bonds. The presence of a broader band around  $1,550 \text{ cm}^{-1}$  of very low intensity can be attributed to the presence of graphitic carbon impurities ( $\text{sp}^2$  carbon) contamination. The ratio of graphite to the diamond scattering intensities ( $I_{1,590}/I_{1,330}$ ) counts is very low ( $<0.05$ ), and it is in agreement with the literature describing high-quality BDD films [22], thus revealing that only a very small amount of impurity is presented after the BDD preparation via HFCVD using ethanol as source of carbon. This result shows that ethanol can significantly decrease the graphitic carbon impurities in situ, differently of the others sources.

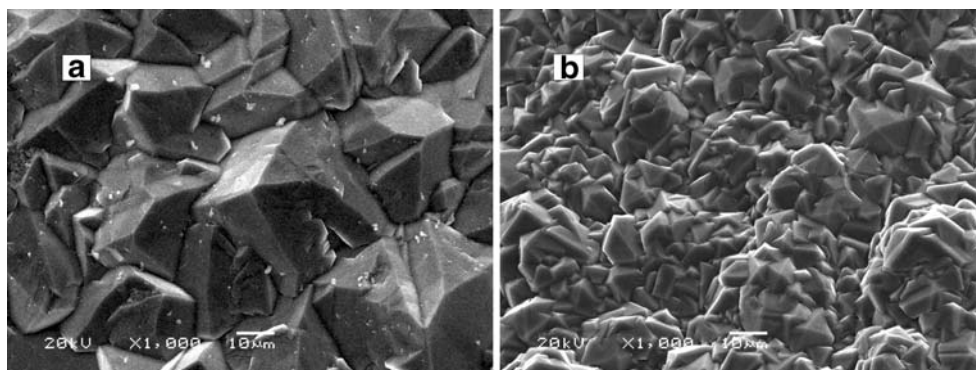
### SEM analysis

Figure 2 shows the typical SEM images of polycrystalline BDD films of types A (Fig. 2a) and B (Fig. 2b), respectively. Grains of an average size of  $36\text{--}21 \text{ }\mu\text{m}$  for type A (Fig. 2a)



**Fig. 1** Typical Raman spectra of “as-grown” boron-doped diamond: solid line, type A; dashed line, type B

**Fig. 2** SEM images of polycrystalline BDD films: **a** type A; **b** type B



and 8–4.5  $\mu\text{m}$  for type B (Fig. 2b) are clearly observed. The SEM images show the tungsten-supported polycrystalline BDD films are mainly characterized by a uniform distribution of homogenous grains. Each grain presents a well-defined, randomly oriented appearance. In addition, the diamond films are without noticeable cracks, thus ensuring the necessary protection of the tungsten support for electrochemical applications. As discussed by Pleskov [3], BDD films not only withstand corrosion, but they protect the metal substrate against chemical attack.

#### Electrochemical characterization

Cathodic treatments were carried out to improve the charge transfer of the “as-grown” diamonds. The cyclic voltammograms are presented in Fig. 3. It can be observed that a significant increase in the electron transfer is obtained for two samples.

Recently, it was found that the carrier density near to the BDD electrode surface may be controlled by changing surface terminations [23]. The hydrogen-terminated diamond shows p-type semiconductivity with holes strongly limited to the surface region [24]. Hydrogenated samples exhibit a p-type conductivity, with an activation energy one order of magnitude lower than that of boron. Several models have been proposed for the source of conductivity. One suggestion is that hydrogen is directly responsible for the acceptor level [25]. A more likely model involves the transfer of electrons from the diamond to surface adsorbates [26], but the experimental evidence is far from clear. As a final point, it has been suggested that hydrogen is added by self-traps implantation, implying the simultaneous formation of an immobile hydrogen aggregate or a lattice defect [27]. We suppose that during the cathodic treatment, the generated hydrogen species are trapped on a boron acceptor on the surface of the diamond, in this manner there is the hole generation process, and thus the conductivity can be correlated by the presence of a hydrogenated surface. Different works have shown that BDD with a hydrogen-terminated surface is, generally, the most active and gives the most reproducible response [4, 7, 8]. In this study, diamonds

with surfaces with very low quantities of nondiamond carbon phases and hydrogen terminated were electrochemically characterized.

Background cyclic voltammograms can be very informative about diamond quality and electrical conductivity [28]. The presence of nondiamond carbon impurity at the surface can be detected, with higher sensitivity than Raman, from background cycling in a strong acid media, especially with the effect on the width of the potential domain where the electrode is ideally polarizable. The background for types A and B electrodes are featureless, low, and ideally polarizable in the respective potential ranges and electrolytes: (1)  $-650$ – $1,780$  and  $-950$ – $2,025$  mV in  $0.1 \text{ mol L}^{-1} \text{ H}_2\text{SO}_4$  solution and (2)  $-820$ – $2,080$  and  $-880$ – $2,110$  mV in  $1 \text{ mol L}^{-1} \text{ HNO}_3$  solution (see Fig. 4).

The exposed geometric areas were  $0.030$  and  $0.036 \text{ cm}^2$  for types A and B electrodes, respectively, and all currents were normalized to these areas. The working potential window obtained from the CV profiles are  $3.28$  and  $3.5 \text{ V}$  ( $\pm 300 \mu\text{A cm}^{-2}$ ) in  $\text{H}_2\text{SO}_4$  and  $4.27$  and  $3.83 \text{ V}$  ( $\pm 9.0 \text{ A cm}^{-2}$ )

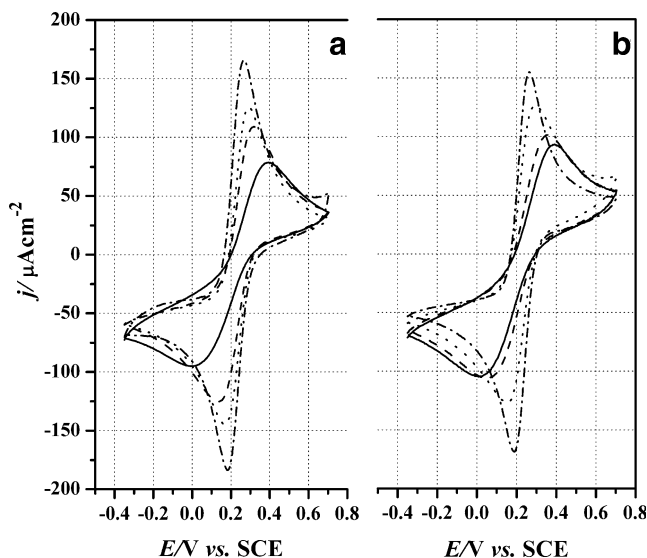


**Fig. 3** Cyclic voltammograms at  $100 \text{ mV s}^{-1}$  for  $1 \times 10^{-3} \text{ mol L}^{-1}$  ferrocyanide in  $0.1 \text{ mol L}^{-1} \text{ KCl}$ , solid line, “as-grown”; cathodic treatments: dashed line, 1, dotted line, 2, dash-dot line, 3, respectively, in electrodes type A (a) and type B (b)

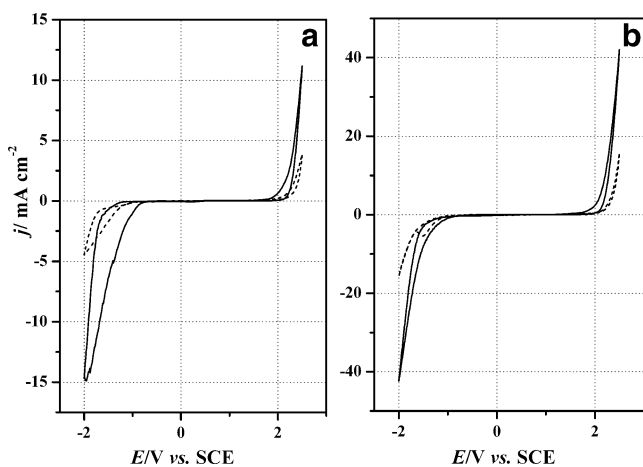


**Fig. 4** Cyclic voltammograms as functions of the electrolyte composition. **a**  $0.1 \text{ mol L}^{-1} \text{ H}_2\text{SO}_4$ ; **b**  $1 \text{ mol L}^{-1} \text{ HNO}_3$  for electrodes type A (solid line) and type B (dashed line). Scan rate:  $100 \text{ mV s}^{-1}$

in  $\text{HNO}_3$  for types A and B electrodes, respectively. The potential window can be related, in part, to the lower fraction of exposed grain boundaries [4]. The electrodes of type B showed to have a larger potential window, presenting a lower fraction of exposed grain boundaries, which is in agreement to the literature [4]. The voltammograms also indicate that no significant level of nondiamond carbon impurities is present.

Cyclic voltammetry was also used to study the electrode response for different redox couples ( $\text{Fe}(\text{CN})_6^{3-/4-}$ ,  $\text{Ru}(\text{NH}_3)_6^{3+/2+}$ ) and for dopamine. These redox systems were chosen because several works with  $\text{sp}^2$  carbon (e.g., graphite, glassy carbon, etc.) and doped  $\text{sp}^3$  carbon (e.g., diamond) have used them [4, 7, 28–30]. In this study, the heterogeneous electron-transfer reactions were considered because the extent to the physicochemical properties of  $\text{sp}^2$  and  $\text{sp}^3$  carbon electrodes influence the response depends on the mechanistic aspects for the particular redox analyte [4, 8, 31].

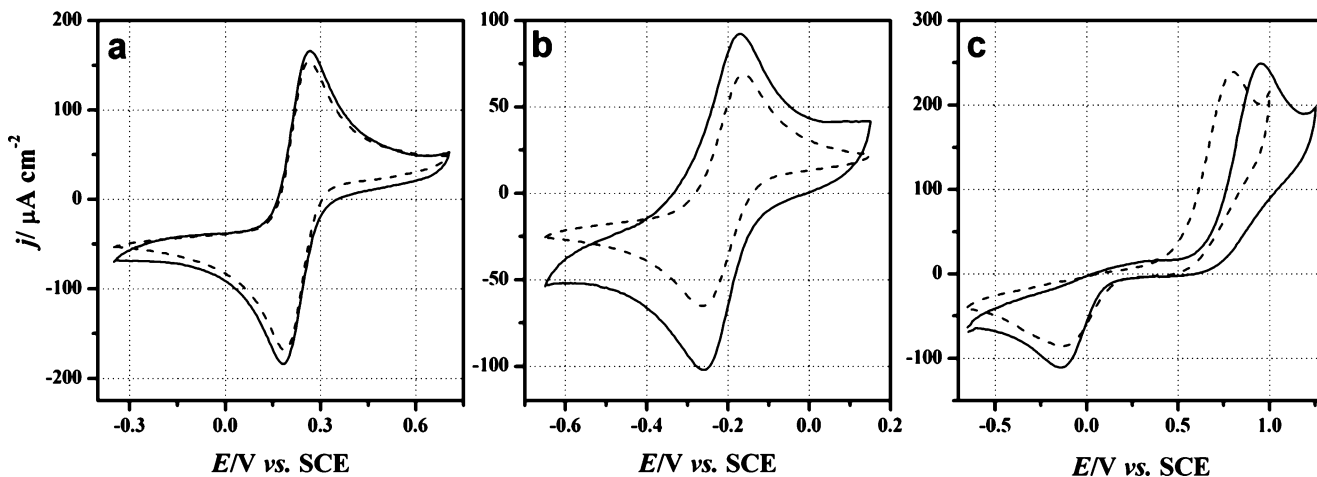


**Fig. 5** Cyclic voltammograms for three analytes: ferrocyanide (a), hexamineruthenium (b) and dopamine (c) at BDD type A (solid line) and type B (dashed line) electrodes. All redox analyte concentrations

The ferri/ferrocyanide system was chosen because it is also well known to be highly sensitive to surface chemical groups on carbon electrodes [4, 6, 22]. The surface chemical effect responsible for the low kinetics of the  $\text{Fe}(\text{CN})_6^{3-/4-}$  redox reaction is directly related to the carbon–oxygen functionalities because of the presence of graphitic microdomains (carbon  $\text{sp}^2$ ) or the activation of these microdomains during the anodic polarization [4, 6, 7]. Granger and Swain [6] have shown that cyclic voltammetric curves are much more reversible after acid washing followed by surface rehydrogenation. After these treating, the removal of the carbon  $\text{sp}^2$  is expected [4, 6]. The reactivity of the BDD electrode to the ferri/ferrocyanide system is also re-established because such reactivity is strongly associated with p-type surface conductivity, in which the hole generation process is correlated by the presence of a hydrogenated surface [4, 6, 7].

Mahé et al. [7] showed that a drastic electrochemical polarization can clean the graphitic microdomains and accomplish the rehydrogenation of the surface, contributing to an increase in the kinetics of the redox reaction of  $\text{Fe}(\text{CN})_6^{3-/4-}$ . Thus, some authors have been reactivating the surface through cathodic treatments [7, 22, 23]. In this work, a significant improvement in the electron transfer for the ferri/ferrocyanide system after a mild cathodic treating was also verified (see Fig. 3). In the literature [6], the values of the heterogeneous electron-transfer rate constant  $k^0$  vary from  $10^{-5}$  to  $10^{-2} \text{ cm s}^{-1}$  for the case of a BDD electrode.

The reduction of  $\text{Ru}(\text{NH}_3)_6^{3+/2+}$  is also commonly used to characterize the quality and properties of a diamond film and allows the comparison with data obtained in electrochemical experiments with other types of diamond and carbon electrode materials [1]. The electrode kinetics for  $\text{Ru}(\text{NH}_3)_6^{3+/2+}$  are relatively insensitive to the surface microstructure, surface oxides, and adsorbed monolayers on  $\text{sp}^2$  carbon electrodes [5, 32]. The most important factor affecting the reaction rate is the electronic properties of the

were  $10^{-3} \text{ mol L}^{-1}$ . The supporting electrolyte was  $1 \text{ mol L}^{-1} \text{ KCl}$ . Scan rate:  $100 \text{ mV s}^{-1}$

electrode, specifically the density of electronic states close to the formal potential of the redox system [4]. Heterogeneous electron-transfer rate constants between 0.01 and  $0.2 \text{ cm s}^{-1}$  are commonly observed for conducting polycrystalline films with extensive pretreatment [4, 8, 28].

Dopamine exhibits much more electrochemical irreversibility, as evidenced by the relatively large  $\Delta E_p$ . This more irreversible behavior is characteristic of all the catechols and catecholamines investigated so far on diamond electrodes [2, 4, 33, 34]. The value of  $k^0$  for dopamine, as well as for other catecholamines, the electron-transfer reaction on the BDD electrode surface, resides in the  $10^{-4}$  to  $10^{-5} \text{ cm s}^{-1}$  interval [4].

Figure 5 shows CV obtained for different electron-transfer reactions taking place at the BDD electrode.

The kinetic parameters for the system  $\text{Fe}(\text{CN})_6^{3-/4-}$  and  $\text{Ru}(\text{NH}_3)_6^{3+/2+}$  were obtained according to Nicholson's method [35], assuming a value of the cathodic electron transfer coefficient  $\alpha=0.5$  and diffusion coefficients for oxidized ( $D_{\text{Ox}}$ ) and reduced species ( $D_{\text{Red}}$ ) in  $1 \text{ mol L}^{-1}$  KCl.

In all cases, the CV profiles furnished a linear response for the dependence of the peak current on the root of the scan rate, thus revealing that the voltammetric current is controlled by the semi-infinite linear diffusion of the redox species at the BDD/solution interface. In the special case of dopamine, the kinetic parameter was obtained from the Tafel plot ( $E$  vs  $\log i$ ) because of the irreversible behavior presented by this compound. CV and kinetic parameters are presented in Table 1.

The results presented in Table 1 are coherent with those found in the literature [4, 6, 7, 28]. In a comparative analysis among the electrodes, the  $\Delta E_p$  values are smaller for type B electrodes, which supplied larger  $k^0$  values. Although type A presented smaller values of  $k^0$  in relation to type B, such electrodes are within the standard parameters for electroanalytical purposes. On the other hand, note that the oxidation current was larger for type A electrodes for all analytes, indicating a higher sensitivity. Electrodes prepared from ethanol as the carbon source showed excellent electrochemical parameters and thus become an alternative to diamond electrodes produced with methane.

*Electrochemical impedance spectroscopy* As previously discussed by Mahé et al. [7], the electrochemical kinetic

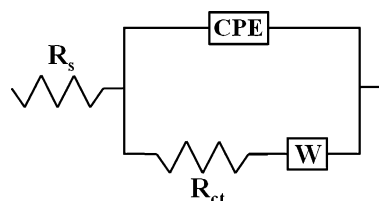


**Fig. 6** Equivalent circuit used for representing the impedance response in the presence of diffusion control

parameters determined using EIS are more reliable than those from CV because EIS constitutes a more efficient and more accurate experimental approach than CV. Therefore, in the present case, we have performed EIS analysis to compare the results with those obtained from CV.

EIS analysis of BDD electrodes can be carried out in the presence of diffusion control using the Randles–Ershler's circuit presented in Fig. 6 [3, 7].

In the equivalent circuit,  $R_s$  is the uncompensated ohmic resistance ( $=R_{\text{solution}}$ ); CPE is the constant phase element used for representing the capacitive behavior presented by the double layer capacitance;  $R_{ct}$  is the charge transfer resistance, and  $W$  is the Warburg impedance associated with diffusion control at the BDD/solution interface.

Using the treatment proposed by Brug et al. [36], the double layer capacitance  $C_{dl}$  was obtained from the CPE using the equation:

$$C_{dl}^{\phi} = \frac{Z_{\text{CPE}}^{-1}(j\omega)^{-\phi}}{\left[(R_s)^{-1} + (R_{ct})^{-1}\right]^{(1-\phi)}} \quad (1)$$

where the parameters are obtained from impedance data using the complex nonlinear least square fitting (CNLS) [21]. The power  $\phi$  is a dimensionless parameter related to the depression angle originated from the non-ideal electric behaviour presented by any electrode/electrolyte interface.

In the present case, the EIS study was carried out in a solutions having a  $10^{-3} \text{ mol L}^{-1}$  concentration of the different redox systems ( $\text{Fe}(\text{CN})_6^{3-/4-}$ ,  $\text{Ru}(\text{NH}_3)_6^{3+/2+}$  or dopamine) under natural convection, using  $1 \text{ mol L}^{-1}$  KCl as the supporting electrolyte. In all cases, the EIS spectrum was recorded at the open circuit potential (equilibrium potential), which for the type A and B BDD electrodes and the  $\text{Fe}(\text{CN})_6^{3-/4-}$ ,  $\text{Ru}(\text{NH}_3)_6^{3+/2+}$  and dopamine systems, were 223/226, -233/-153, and 809/636 mV(vs SCE), respectively.

**Table 1** CV and kinetic parameters obtained at BDD type A and type B electrodes for three redox systems in  $1 \text{ mol L}^{-1}$  KCl at  $25^\circ \text{C}$

BDD type	$\Delta E_p$ (mV)		$I_p^a$ ( $\mu\text{A cm}^{-2}$ )		$I_p^a/I_p^c$		$k^0$ ( $\text{cm s}^{-1}$ )		$\alpha$	
	A	B	A	B	A	B	A	B	A	B
$\text{Fe}(\text{CN})_6^{3-/4-}$	83.0	68.0	174.27	166.11	1.04	0.99	0.010	0.028	0.50	0.50
$\text{Ru}(\text{NH}_3)_6^{3+/2+}$	92.0	92.0	92.33	68.06	0.90	1.07	0.008	0.008	0.50	0.50
Dopamine	804.0	648.0	133.27	101.11	1.66	1.54	$2.08 \times 10^{-5}$	$6.60 \times 10^{-5}$	0.24	0.22

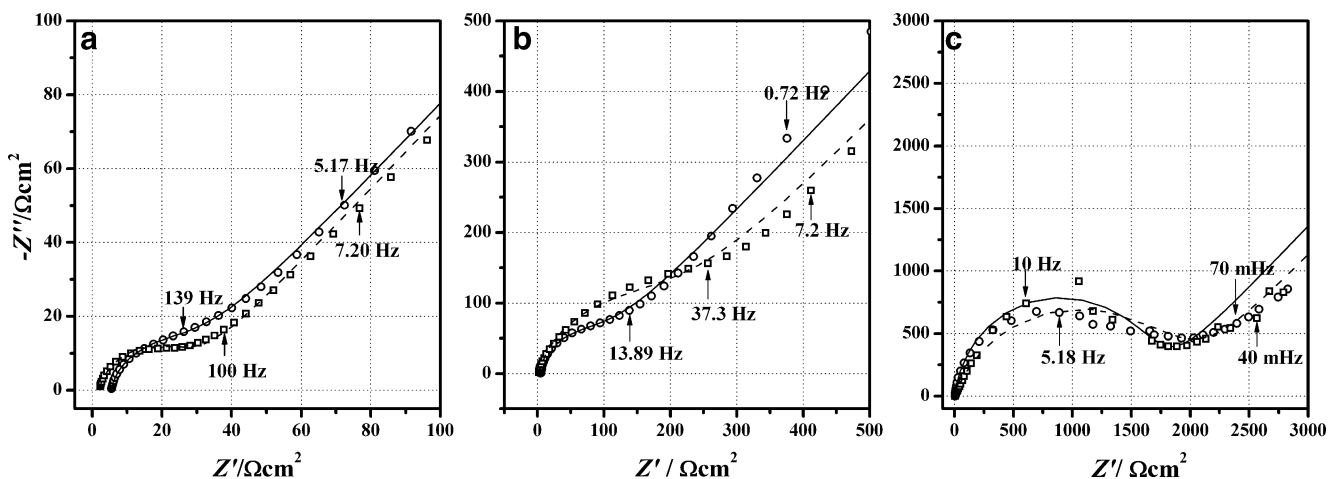


**Fig. 7** Nyquist plots obtained for different electron-transfer reactions on BDD electrodes: **a** ferrocyanide,  $10^{-3} \text{ mol L}^{-1}$ ; **b** hexamineruthenium,  $10^{-3} \text{ mol L}^{-1}$ ; **c** dopamine,  $10^{-3} \text{ mol L}^{-1}$ . Supporting electrolyte

was  $1.0 \text{ mol L}^{-1} \text{ KCl}$ .  $T=25 \text{ }^\circ\text{C}$ . Legend: Type A, experimental (circles) and curve fitting (solid line); type B, experimental (squares) and curve fitting (dashed line)

Figure 7 shows Nyquist plots obtained for the type A and type B electrodes as functions of the solution composition.

Analyzing Fig. 7 reveals that both electrode preparation conditions and the solution composition considerably affect the electrochemical response of BDD electrodes in the frequency domain. The behavior of the impedance spectra displayed in Fig. 7a and b, which were obtained for the  $\text{Fe}(\text{CN})_6^{3-/4-}$  and  $\text{Ru}(\text{NH}_3)_6^{3+/2+}$  redox couples, respectively, supports a typical diffusion-controlled process, mainly characterized by a slight deviation from the ideal reversible case, thus showing quasi-reversible behaviors. As a result, the analysis fit via CNLS revealed a good correspondence in these cases. In the special case of dopamine, the impedance data are considerably different from the ones already described. A qualitative analysis of these findings indicated a considerable deviation from the ideal reversible case, as expected.

The heterogeneous electron-transfer rate constant  $k^0$  at the equilibrium potential can be obtained from the  $R_{ct}$  values (available from the CNLS fit) according to Eq. 2:

$$k^0 = \frac{RT}{n^2 F^2 R_{ct} C} \quad (2)$$

The parameters presented in Eq. 2 have their usual significance.

A summary of results obtained by EIS are presented in Table 2.

Comparing the results listed in Tables 1 and 2, it is clearly observed that the EIS technique provided  $k^0$  values slightly different. This discrepancy probably finds its origin in the different accuracies presented by the CV and EIS techniques [7].

The standard electrochemical behavior of high-quality BDD electrodes, in the presence of different redox systems, was reported by Granger et al. [4]. These authors found that the  $\text{Fe}(\text{CN})_6^{3-/4-}$  redox couple undergoes electron transfer that is extremely sensitive to the surface chemistry of BDD, thus reporting  $k^0$  in the range of  $10^{-2}$ – $10^{-1} \text{ cm s}^{-1}$ . According to the literature [7] for BDD electrodes, the electrochemical reactivity for the  $\text{Fe}(\text{CN})_6^{3-/4-}$  system is considerably affected by the p-type surface conductivity in which the hole generation process is correlated by the presence of an hydrogenated surface.

Granger et al. [4] also found that the  $\text{Ru}(\text{NH}_3)_6^{3+/2+}$  redox couple is mainly characterized by an electron transfer that is insensitive to the diamond surface microstructure and chemistry with  $k^0$  in the  $10^{-2}$ – $10^{-1} \text{ cm s}^{-1}$  range. Besides,

**Table 2** The double-layer capacity  $C_{dl}$  and the heterogeneous electron-transfer rate constant  $k^0$  for BDD type A and type B electrodes obtained from the EIS data for different redox systems

BDD type	$k^0 \text{ (cm s}^{-1}\text{)}$		$C_{dl} \text{ (}\mu\text{F cm}^{-2}\text{)}$		$\phi$	
	A	B	A	B	A	B
$\text{Fe}(\text{CN})_6^{3-/4-}$	0.015	0.010	5.87	0.76	0.88	0.84
$\text{Ru}(\text{NH}_3)_6^{3+/2+}$	$2.99 \times 10^{-3}$	$1.31 \times 10^{-3}$	8.90	0.56	0.95	0.84
Dopamine	$1.70 \times 10^{-4}$	$1.46 \times 10^{-4}$	5.56	5.64	0.91	0.92

Supporting electrolyte:  $1.0 \text{ mol L}^{-1} \text{ KCl}$ .  $T=25 \text{ }^\circ\text{C}$

according to this report, dopamine undergoes sluggish electron transfer with  $k^0$  between  $10^{-4}$  and  $10^{-5}$  cm s<sup>-1</sup>.

A comparison of the findings discussed above with the results in Table 2 shows a rather good correspondence, thus revealing that the electrochemical properties of our BDD films are very similar to those ones pertaining to the high-quality BDD electrodes reported in the literature.

Table 2 shows double-layer capacitance values, in the range of 0.56–8.90  $\mu\text{F cm}^{-2}$ . These values are in agreement with the ones presented by Mahé et al. [7], who reported a capacitance of 2.5  $\mu\text{F cm}^{-2}$  in the case of  $\text{Fe}(\text{CN})_6^{3-/4-}$ . Therefore, based on the discussion presented by these authors [7], it can be argued that both electrodes are adequate for analytical applications. However, it is worthwhile to mention that the type B presents better characteristics because of its lower capacitance.

Analysis of the capacitance data presented in Table 2 also reveals that the influence of the electrode preparation conditions is more pronounced in the case of the  $\text{Fe}(\text{CN})_6^{3-/4-}$  redox couple, while in the case of  $\text{Ru}(\text{NH}_3)_6^{3+/2+}$  and dopamine, it is observed that the value remained approximately constant. This behavior is in agreement with the literature [4], where it was found that the  $\text{Ru}(\text{NH}_3)_6^{3+/2+}$  redox couple is less sensitive to the BDD surface microstructure than is the  $\text{Fe}(\text{CN})_6^{3-/4-}$  system.

Any possible influence on the electrode behavior promoted by changes in the semiconductor properties during the CVD process using ethanol as a carbon source would appear by the change in the electrochemical behavior of BDD for “standard” redox reactions (e.g., outer and inner sphere redox processes). Thus the developed BDD electrodes present similar electronic properties when comparing with the BDD electrodes currently found in the literature.

## Conclusions

BDD film electrodes grown from the ethanol carbon source presented improved electrochemical properties because ethanol can decrease significantly the graphitic carbon impurities in situ, differently from the others sources. Hence, a great number of electrochemical technologies could benefit from the use of this electrode material such, as: electroanalysis, electrocatalysis, electrooxidation, spectroelectrochemistry, and bioelectrochemistry. The conclusions of this work allow emphasis on several points: (1) Ethanol is an excellent alternative source of carbon for growing BDD films for electrochemical applications; (2) a mild cathodic treatment caused significant increases in the electron transfer; (3) Raman reveals that only a very small amount of nondiamond carbon impurity was itself formed at the BDD film using ethanol as a source of carbon; (4)

both type A and type B samples had similar morphologies, although their grain sizes are different because of the different deposition temperatures; (5) the background for type A and type B electrodes is low, featureless, and ideally polarizable indicating, again, that no significant level of nondiamond carbon impurities is present; and (6) according to investigations from several aqueous-based redox systems using CV and EIS, it could be noticed that the electrochemical parameters for the same technique attributed to both films are similar. However, small differences occur in the parameters between the techniques. From our point of view, EIS is a much more accurate technique, compared to CV, because of its more direct way in obtaining the system information; (7) the behavior of the EI spectra for  $\text{Fe}(\text{CN})_6^{3-/4-}$  and  $\text{Ru}(\text{NH}_3)_6^{3+/2+}$  redox couples supports a typical diffusion-controlled process. In the special case of dopamine, a considerable deviation from the ideal reversible case happened, possibly because of the absence of carbonyl surface functionalities on the hydrogen-terminated surface; (8) the resulting capacitance values for both types of electrodes indicate that these BDD electrodes are promising for analytical application.

**Acknowledgments** We thank Prof. Carol Collins for her technical assistance in English and the “Grupo de Propriedades Ópticas” of IFGW/UNICAMP for use of their Raman spectrometer. We also gratefully acknowledge the Brazilian agencies FAPESP, CAPES, and CNPq for partial financial support.

## References

- Goeting CH, Foord JS, Marken F, Compton RG (1999) *Diamond Relat Mater* 8:824
- Xu JS, Granger MC, Chen QY, Strojek JW, Lister TE, Swain GM (1997) *Anal Chem* 69:A591
- Pleskov YV (2002) *Russ J Electrochem* 38:1275
- Granger MC, Witek M, Xu JS, Wang J, Hupert M, Hanks A, Koppang MD, Butler JE, Lucazeau G, Mermoux M, Strojek JW, Swain GM (2000) *Anal Chem* 72:3793
- Ranganathan S, Kuo TC, McCreery RL (1999) *Anal Chem* 71:3574
- Granger MC, Swain GM (1999) *J Electrochem Soc* 146:4551
- Mahé E, Devilliers D, Comninellis C (2005) *Electrochim Acta* 50:2263
- Hupert M, Muck A, Wang R, Stotter J, Cvackova Z, Haymond S, Show Y, Swain GM (2003) *Diamond Relat Mater* 12:1940
- Stoneham AM, Ford IJ, Chalker PR (1998) *MRS Bull* 23:28
- Shah SI, Waite MM (1992) *Appl Phys Lett* 61:3113
- Ruan J, Choyke WJ, Kobashi K (1993) *Appl Phys Lett* 62:1379
- Baranauskas V, Tosin MC, Peterlevitz AC, Ceragioli H, Durrant SF (2000) *J Appl Phys* 88:1650
- Baranauskas V, Li BB, Peterlevitz A, Tosin MC, Durrant SF (1999) *J Appl Phys* 85:7455
- Su QF, Lu JF, Wang LJ, Liu JM, Ruan JF, Cui JT, Shi WM, Xia YB (2005) *Solid-State Electron* 49:1044
- Ma ZB, Wang JH, Wang CX, Man WD (2003) *Plasma Sci Technol* 5:1735
- Li BB, Baranauskas V, Peterlevitz A, Chang DC, Doi I, Trava-Airoldi VJ, Corat EJ (1998) *Diamond Relat Mater* 7:1259

17. Honda K, Yoshimura M, Rao TN, Tryk DA, Fujishima A, Yasui K, Sakamoto Y, Nishio K, Masuda H (2001) *J Electroanal Chem* 514:35
18. Farabaugh EN, Robins L, Feldman A, Johnson CE (1995) *J Mater Res* 10:1448
19. Baranauskas V, Peled A, Trava-Airoldi VJ, Lima C, Doi I, Corat EJ (1994) *Appl Surf Sci* 80:129
20. Marken F, Paddon CA, Asogan D (2002) *Electrochem Commun* 4:62
21. Boukamp BA (1986) *Solid State Ionics* 20:31
22. Ferro S, De Battisti A (2002) *Electrochim Acta* 47:1641
23. Kawarada H (1996) *Surf Sci Rep* 26:205
24. Shinagawa H, Kido G, Takamasu T, Gamo MN, Ando T (2002) *Superlattices Microstruct* 32:289
25. Looi HJ, Jackman RB, Foord JS (1998) *Appl Phys Lett* 72:353
26. Ristein J, Maier F, Riedel M, Stammer M, Ley L (2001) *Diamond Relat Mater* 10:416
27. Goss JP, Jones R, Heggie MI, Ewels CP, Briddon PR, Oberg S (2002) *Phys Rev B* 65:115207
28. Fischer AE, Show Y, Swain GM (2004) *Anal Chem* 76:2553
29. Yang HH, McCreery RL (1999) *Anal Chem* 71:4081
30. DuVall SH, McCreery RL (2000) *J Am Chem Soc* 122:6759
31. Chen PH, Fryling MA, McCreery RL (1995) *Anal Chem* 67:3115
32. Chen PH, McCreery RL (1996) *Anal Chem* 68:3958
33. Fujishima A, Rao TN, Popa E, Sarada BV, Yagi I, Tryk DA (1999) *J Electroanal Chem* 473:179
34. Alehashem S, Chambers F, Strojek JW, Swain GM, Ramesham R (1995) *Anal Chem* 67:2812
35. Nicholson RS (1965) *Anal Chem* 37:1351
36. Brug GJ, Vandeneeden A, Sluytersrehabach M, Sluyters JH (1984) *J Electroanal Chem* 176:275